J. Fluid Mech. (1981), *vol.* 103, *pp.* 257–273
Printed in Great Britain

Linearized thin-wing theory of gas-centrifuge scoops

By TAKEO SAKURAI
Department of Aeronautical Engineering, Faculty of Engineering, Kyoto University

(Received 28 August 1979 and in revised form 19 December 1979)

We study a steady hypersonic rotating flow of a perfect gas past a system of thin stationary scoops in a gas centrifuge of annulus type. The gas is assumed inviscid; its ratio of specific heats is assumed to be approximately 1.

The scoops are set at zero angle of attack and are periodic with respect to the azimuthal variable. The flow is assumed to be a three-dimensional small perturbation on a basic state of rigid-body rotation. New scaling laws are proposed as appropriate to realistic operating conditions of gas centrifuges. Basic equations, boundary conditions and shock conditions are linearized for a weakly hypersonic flow by an analytical procedure similar to that used in the thin-wing approximation in high speed aerodynamics. The solution of the basic equations is obtained by the eigenfunction expansion method. The solution provides us a simple addition theorem for the scoop drag which makes the resultant drag of a system of several scoops equal to the product of the number of scoops and the drag of a standard system with a single scoop. The solution makes it clear that despite the above addition theorem, the scoops interact in their effects on the flow.

1. Introduction

From a gasdynamic viewpoint, scoops in Zippe-type gas centrifuges (Zippe 1960) are stationary bodies placed in a hypersonic rotating stratified flow. Scoop flow has been studied hitherto by an axisymmetric model with differentially rotating disks (see, for example, Hultgren 1978; Landahl 1977; Matsuda & Hashimoto 1976; Schmidt 1972). This model gives us insight into the way a scoop affects meridional circulation. Also there is a numerical study of three-dimensional flow around an obstacle by Elsholz (1977). Cenedese & Cunsolo (1979) proposed a model of three-dimensional structure of the scoop flow. Suzuki & Mikami (1979) made an experimental study of a scoop flow for cases of slow rotation. As obstacles in a hypersonic flow, however, the scoops are expected to induce a system of shock waves which penetrate far into much of the interior of the flow. These waves cause the flow field to be far from axisymmetric. The drag force experienced by the scoops is balanced by the spin-down torque on the rotating cylinder of the centrifuge. Also entropy jumps across shock waves cause an irreversible radial motion of gas particles. To understand these aspects quantitatively, it is necessary to establish for a scoop flow a model that is not axisymmetric.

The purpose of this paper is to give a linearized thin-wing theory of scoops for weakly hypersonic flows by which the axially unsymmetric aspects of scoop flows mentioned above can be predicted analytically.

Let us look at operating conditions of gas centrifuges which can be expected on the

0022–1120/81/4666–3530 $02.00

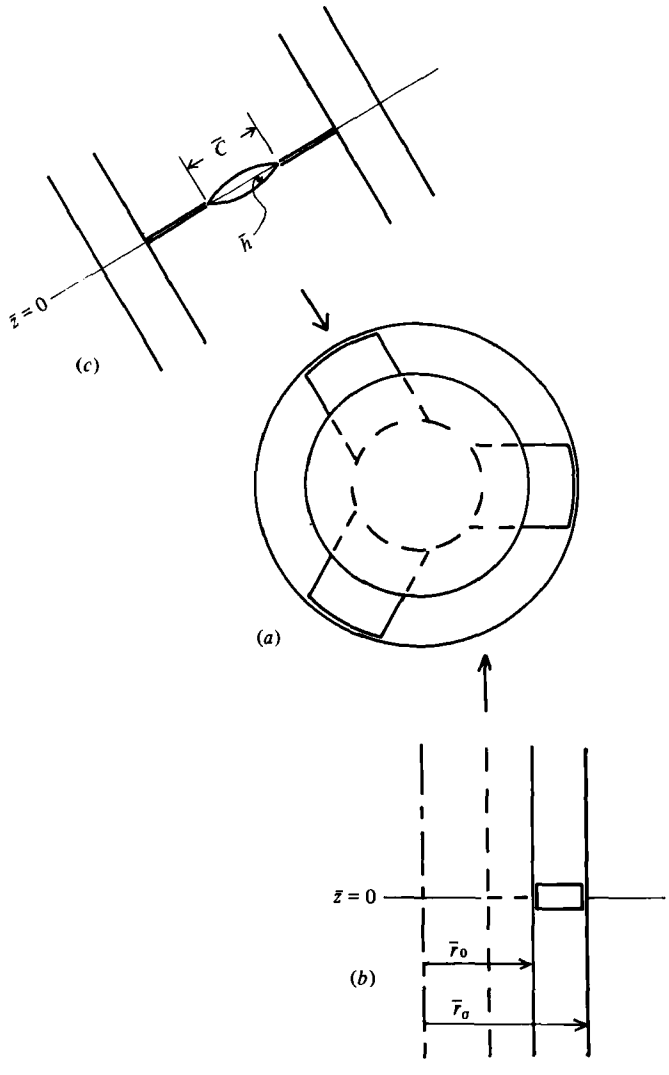

FIGURE 1. Geometry of the scoop mounting: (*a*) planform of the mounting, in which the breadth of the scoop is exaggerated for clarity; (*b*) front view of the scoop; (*c*) side view of the scoop.

basis of data published by Zippe (1960). The radius and the height of the centrifuge are 10 and 400 cm, respectively, the peripheral speed is 500–800 m s^{-1} and the chord length of the scoop as an aerofoil is 1 cm. Because the sound speed at room temperature in UF_6 is 90 m s^{-1}, the above peripheral speeds correspond to Mach numbers 5·6–8·9. For a monatomic or diatomic gas, a flow having this range of Mach numbers has so large a kinetic energy that the gas temperature rises to 1000 K or higher behind a shock front (Chernyi 1961, pp. 1–16; Hayes & Probstein 1966, pp. 1–31). The effects of dissociation of the gas molecules become important in such circumstances. Because UF_6 is multimolecular, the ratio of its specific heats is nearly 1 (in fact it is 1·07); the temperature rise behind a shock front is thus not very large and the effect of dissociation may therefore be neglected. The Reynolds number with respect to the peri-

pheral density and speed and the chord length of the scoop is of the order of 10^{10}. The effects of viscosity can thus be neglected. The contribution of a small segment of the scoop to the local drag is proportional to the local density which decreases rapidly with increasing distance from the periphery. Thus to estimate the total drag on the scoop, we need consider only the region near the periphery. Finally, the chord length of the scoop can be taken to be of the order of the cylinder radius divided by the peripheral Mach number.

In accord with the above parameter survey, let us consider a narrow annulus bounded by two concentric circular cylinders of infinite length which rotate with the same angular velocity (see figure 1). The inner cylinder is divided into two parts by a plane gap of infinitesimal width which is perpendicular to the stationary axis of rotation. The chord length of the scoop is of the order of the cylinder radius divided by the Mach number. The scoop has sharp edges, is symmetric with respect to its chord line and has an infinitesimal thickness ratio. The scoops are attached rigidly to the stationary axis by infinitesimally thin plates through the gap. The angle of attack of the scoop is zero with respect to the azimuthal direction. The plan form of the mounting is periodic with respect to the azimuthal variable (see figure 1). The annulus is filled with an inviscid perfect gas whose ratio of specific heats is only slightly greater than 1. The basic flow is a rigid body rotation at the angular velocity of the cylinders. The peripheral Mach number is much larger than 1 and the distance between cylinders is several times the radial density scale height. We restrict our study to a continuum treatment and to weakly hypersonic flow: The effect of the scoops is taken as being a small disturbance of this basic state, or putting it in another way, we regard the rigid body rotation as a 'free stream' in which the thin stationary scoops are immersed periodically. The flow is analysed by a method similar to the linearized thin wing theory in high speed aerodynamics (see Chernyi 1961, pp. 161–171, and Hayes & Probstein 1966, pp. 45–54, for the applicability of thin wing theory to a weakly hypersonic flow).

Before detailed discussion of the analysis, let us survey physical aspects of the scoop flow qualitatively. Because the spanwise direction of the scoop is parallel to the centrifugal acceleration, the scoop flow is similar to river flow past a pier of a bridge. In the case of a river, the horizontal acceleration resulting from the blocking effect of a pier causes vertical acceleration in virtue of Bernoulli's relation. In the case of the scoop flow, the azimuthal component of the velocity changes as the gas flows past the scoop. This 'horizontal' variation of velocity causes the temperature and hence also the density of the gas to vary and therefore the centrifugal acceleration gives rise in turn to a radial motion. Because the configuration is periodic, the disturbance caused near the scoop trails downstream to influence the flow around the other scoops and to feed back to the flow around the original scoop. The most interesting product of the present study, however, is a simple addition theorem for the resultant drag of the scoop system, despite the interaction between scoops. Let us compare a system A of n scoops with a standard system B having a single scoop. The resultant scoop drag of system A is just n times the scoop drag of system B. This addition theorem agrees well with Zippe's drag experiment (Zippe 1960).

In § 2 basic equations, boundary conditions and shock conditions are discussed on the basis of the linearized thin wing theory in weakly hypersonic flows and new scaling laws are proposed. In § 3 the basic equations are solved by use of an eigenfunction

expansion. In § 4 a new addition theorem for the resultant drag of a system of scoops is derived and some numerical results are given. For clarity the exact basic equations, boundary conditions and shock conditions are given in the appendix.

2. Basic equations and proposed new scaling laws

Let us consider the model shown in figure 1 (see § 1 for detailed explanation). The chord length of the scoop is of the order of the cylinder radius divided by the peripheral Mach number. The distance between the cylinder is of the order of several times the radial density scale heights. The effect of the system of stationary scoops is assumed to be a steady three-dimensional small disturbance superposed on a basic state of rigid-body rotation at uniform temperature.

We now introduce the following dimensionless variables for physical quantities with respect to the rest frame of reference. We expect these quantities to have values of order 1 for the flows we study here:

$$r = (\bar{r}-1)/\epsilon_2, \quad \tilde{r} = \bar{r}/\bar{r}_0, \quad \theta = \bar{\theta} G_{01}, \quad z = \bar{z} G_{02}/(\bar{r}_0 \epsilon_2); \tag{1}$$

$$U = \frac{\bar{q}_r}{\epsilon \bar{V}_0}, \quad V = \frac{(\bar{q}_\theta - \bar{V}_0 \tilde{r})\, G_{01}}{\epsilon \bar{V}_0}, \quad W = \frac{\bar{q}_z}{\epsilon \bar{V}_0}, \quad \bar{V}_0 = \bar{r}_0 \bar{\Omega}; \tag{2}$$

$$\left.\begin{aligned} \rho &= \frac{\bar{\rho}-\bar{\rho}_B}{\epsilon_3 \bar{\rho}_B}, \quad p = \frac{\bar{p}-\bar{p}_B}{\epsilon_3 \bar{p}_B}, \quad T = \frac{\bar{T}-\bar{T}_0}{\epsilon_1 \epsilon_3 \bar{T}_0}, \\ \bar{\rho}_B &= \bar{\rho}_{B0} \exp\left(r + \tfrac{1}{2}\epsilon_2 r^2\right), \quad \bar{p}_B = \bar{\rho}_B \bar{R} \bar{T}; \end{aligned}\right\} \tag{3}$$

$$\left.\begin{aligned} &\epsilon_1 = \gamma - 1, \quad \epsilon_2 = G_0^{-1}, \quad \epsilon_3 = \epsilon G_{01}, \\ &G_{01} = (G_0 \gamma)^{\frac{1}{2}}, \quad G_{02} = 1 - \frac{\epsilon_2}{2}, \quad G_0 = \frac{\bar{r}_0^2 \bar{\Omega}^2}{\bar{R} \bar{T}_0}; \end{aligned}\right\} \tag{4}$$

$$h(\theta) = \bar{h}(\bar{\theta})/(\epsilon \bar{r}_0 G_{01}^{-1}). \tag{5}$$

In the above $(\bar{r}, \bar{\theta}, \bar{z})$ is a system of cylindrical co-ordinates in a rest frame of reference, $(\bar{q}_r, \bar{q}_\theta, \bar{q}_z)$ the velocity, $\bar{\rho}$ the density, $\bar{p}$ the pressure, $\bar{T}$ the temperature, $\bar{\Omega}$ the angular velocity of the cylinder, $\bar{R}$ the gas constant, γ the ratio of the specific heats, and $\bar{h}$ the local height of the scoop surface (see figure 2). The overbars on letters refer to the original dimensional physical quantities ($\bar{\theta}$ is non-dimensional as an exception): $\bar{r}_0$ is the radius of the inner cylinder, $\bar{T}_0$ is the uniform temperature of the basic state.

The suffix B refers to the basic state; $\bar{r}_0 G_{01}^{-1} (= \bar{C})$ in (5) is the chord length of the scoop. The parameter ϵ is the thickness ratio of the scoop. As the parameter survey in § 1 suggests, ϵ_1, ϵ_2 and ϵ are all assumed to be approximately 0·01. It is important to note that the smallness of these parameters stems from different physical causes: ϵ_1 is small for polyatomic gases, ϵ_2 is small for high peripheral velocity on the boundary and ϵ is small for thin scoops. Therefore it makes sense (physically as well as mathematically) to construct an expansion in which ϵ_1, ϵ_2 and ϵ_3 are independent parameters. It is interesting that ϵ_3 is of the same form as the hypersonic similarity parameter, i.e. ϵ_3 is of the order of a multiple of the thickness ratio of the scoop and the Mach number of the flow (Chernyi 1961, pp. 25–54; Hayes & Probstein 1966, pp. 32–47). If ϵ is of the order of 0·1, as may be expected for practical centrifuges, ϵ_3 becomes of the order of 1. Then the flow is hypersonic and the effects of nonlinear terms in the basic equations

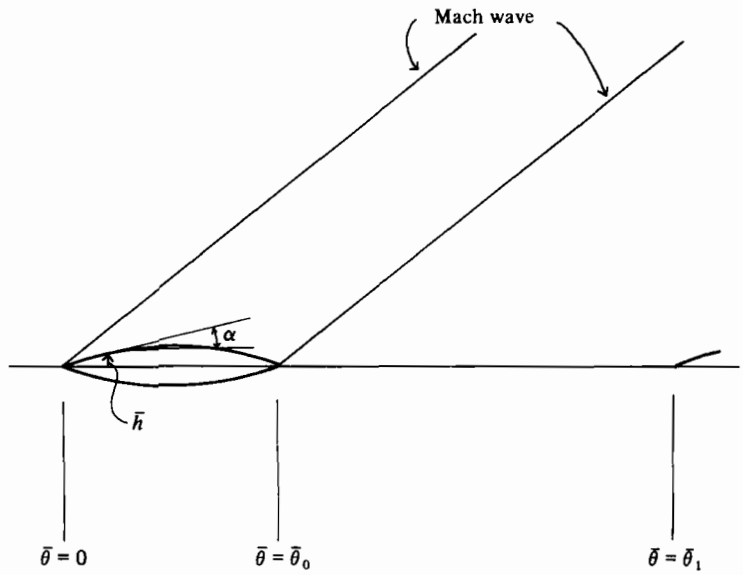

FIGURE 2. $(\bar{\theta}, \bar{z})$ cross-section of the scoop mounting. The chord length of the scoop is $\bar{\theta}_0$ and the spacing between scoops is $\bar{\theta}_1$. Because the distance between the cylinders is small in comparison with the radius, it can be taken as the cross-section at an arbitrary radius.

become important. If ϵ is of the order of 0·01, as is assumed above, ϵ_3 is of the order of 0·1 and is much smaller than 1. The flow is then weakly hypersonic and the usual methods of thin wing expansion theory can be applied (see Ward 1955, pp. 1–31, for the thin wing expansion theory). For simplicity we restrict attention henceforth to weakly hypersonic flow.

We approximate the typical physical quantity q by a linear function of ϵ_1, ϵ_2 and ϵ_3:

$$q = q_0 + \epsilon_1 q_{11} + \epsilon_2 q_{12} + \epsilon_3 q_{13}. \tag{6}$$

We discard terms of order higher than 1 in ϵ_1, ϵ_2 and ϵ_3, and we do not calculate the coefficient q_{13} at all. Substituting (6) into the basic equations and collecting like powers of ϵ_1 and ϵ_2, we obtain the following equations.

Order 0:

$$0 = \rho_{0,\theta} + W_{0,z}, \quad 0 = V_{0,\theta} + p_{0,\theta}, \tag{7), (8}$$

$$0 = W_{0,\theta} + p_{0,z}, \quad p_0 = \rho_0. \tag{9), (10}$$

Order ϵ_1:

$$0 = U_{11} + U_{11,r} + \rho_{11,\theta} + W_{11,z} + \rho_{0,\theta}, \tag{11}$$

$$0 = U_{11,\theta} + p_{11,r} + T_0, \tag{12}$$

$$0 = V_{11,\theta} + p_{11,\theta} + 2U_{11} + p_{0,\theta}, \tag{13}$$

$$0 = W_{11,\theta} + p_{11,z}, \quad 0 = p_{11} - \rho_{11} - T_0, \quad T_0 = \rho_0. \tag{14), (15), (16}$$

Order ϵ_2:

$$0 = U_{12} + U_{12,r} + \rho_{12,\theta} + W_{12,z} + V_{0,\theta} - \frac{W_{0,z}}{2}, \tag{17}$$

$$0 = U_{12,\theta} + p_{12,r} - 2V_0, \quad 0 = V_{12,\theta} + 2U_{12} + p_{12,\theta} - rp_{0,\theta}, \tag{18), (19}$$

$$0 = W_{12,\theta} + p_{12,z} - \tfrac{1}{2}p_{0,z}, \tag{20}$$

$$p_{12} = \rho_{12}. \tag{21}$$

Here a co-ordinate preceded by a comma in the suffix indicates a partial derivative with respect to that co-ordinate. In the equations of order 0, we use the fact that $U_0 = 0$ and $\partial/\partial r = 0$ to omit vanishing terms. The form of these equations is the same as in the linearized theory of two-dimensional supersonic flow. It is to be noted, however, that our approximation of order 0 corresponds to an isothermal situation. Inspection of (7), (8), (9), (10), (12) and (16) indicates that the adiabatic expansion and contraction related with the meridional motion induced by the scoop causes radial motion by the radial buoyancy force subject to the centrifugal acceleration.

Substitution of (6) into boundary conditions on the scoop and on the centrifuge cylinders gives us the following:

Conditions of order 0:

$$W_0|_{z=0} = h_\theta, \quad U_0|_{r=0} = U_0|_{r=r_\sigma} = 0. \tag{22), (23}$$

Conditions of order ϵ_1:

$$W_{11}|_{z=0} = 0, \quad U_{11}|_{r=0} = U_{11}|_{r=r_\sigma} = 0. \tag{24), (25}$$

Conditions of order ϵ_2:

$$W_{12}|_{z=0} = 0, \quad U_{12}|_{r=0} = U_{12}|_{r=r_\sigma} = 0. \tag{26), (27}$$

Here r_σ refers to the outer cylinder, $z = 0$ to the symmetric plane of scoops and subscript θ to differentiation with respect to θ. In (22), h is determined by the shape of the cross-section of the scoop and the form of the mounting. For simplicity we assume that the scoop is mounted at zero angle of attack with respect to the azimuthal variable and that h depends on θ only. The (θ, z) cross-section of the scoop mounting is shown in figure 2.

Because our flow field extends to infinity in the axial direction, we must prescribe an asymptotic behaviour of the solution. In accord with von Kármán's 'zone of action' rule (John 1969), we impose the following conditions on the approximations at each order:

> characteristic surfaces of wave modes of the solution must subtend acute angles from the downstream direction of the basic flow of rigid body rotation. (28)

Substitution of (6) into shock conditions gives us the following conditions.

Shock conditions of order 0:

$$[\rho_0 - W_0] = 0, \quad [V_0 + W_0] = 0, \quad [U_0] = 0. \tag{29), (30), (31}$$

Shock conditions of order ϵ_1:

$$[\rho_{11} - W_{11} + \rho_0] = 0, \quad [V_{11} + W_{11} + W_0] = 0, \quad [U_{11}] = 0. \tag{32), (33), (34}$$

Shock conditions of order ϵ_2:

$$[\rho_{12} - W_{12} + \tfrac{1}{2}V_0] = 0, \quad [V_{12} + W_{12} - rW_0 - \tfrac{1}{2}V_0] = 0, \quad [U_{12}] = 0. \tag{35), (36), (37}$$

Here brackets refer to the jump of the bracketed quantities across the Mach waves of the order 0 (see figure 2 as regards the Mach–wave geometry). In deriving the above, our procedure makes us assume that the shock waves are weak. As is shown

by Ward (1955, pp. 70–72), the normal component of the law of conservation of momentum across the shock front degenerates to the law of conservation of mass and the law of conservation of energy is used to determine the relation between the shock angle and the deflexion angle of the velocity vector. It is interesting that the shock conditions (29)–(37) can also be derived by integrating our equations, order by order, across the Mach waves of zeroth order: $\theta \pm z = \text{const.}$

Our mathematical problem is to solve, for example, equations (11)–(16) subject to the boundary conditions (24), (25) and (28) and the shock conditions (32)–(34). The formulation is completely analogous to that in the linearized supersonic aerofoil theory and the solution can be determined uniquely.

3. Solution of the basic equations

The solution of the problem of order 0 is

$$\rho_0 = p_0 = W_0 = -V_0 = h(\theta - z), \tag{38}$$

where we restrict attention to the upper half of the flow. By the symmetry of the flow, the lower half is readily obtained.

Elimination procedures applied to (11), (12) and (14) give

$$p_{11,r} + p_{11,rr} - p_{11,\theta\theta} + p_{11,zz} = -\rho_0. \tag{39}$$

The shock conditions (29) and (30) show that the right-hand side experiences a jump at the zeroth-order Mach wave. The solution of (39) subject to the boundary conditions (28) is

$$p_{11} = -r\rho_0 + p_{11H}, \quad p_{11H} = \sum_{m,n} R_n(r)\, X^{(p)}_{mn}(\theta, z), \tag{40}$$

where

$$R_n(r) = e^{-\frac{1}{2}r}\left\{\frac{2n\pi}{r_\sigma}\cos n\pi\frac{r}{r_\sigma} + \sin n\pi\frac{r}{r_\sigma}\right\}, \tag{41}$$

$$X^{(p)}_{mn} = \begin{cases} \exp[-\delta_{mn}z]\,(a_{mn}\cos\gamma_m\theta + b_{mn}\sin\gamma_m\theta), & m < m_0, \\ a_{mn}\cos\xi_{mn} + b_{mn}\sin\xi_{mn}, & m_0 < m, \end{cases} \tag{42}$$

$$\xi_{mn} = \gamma_m\theta - \delta_{mn}z, \quad \gamma_m = 2m\pi/\theta_1, \tag{43), (44}$$

$$\delta^2_{mn} = (-1)^j\left\{\frac{r_\sigma^2 + 4n^2\pi^2}{4r_\sigma^2} - \gamma_m^2\right\}, \quad j = \begin{cases} 0, & m < m_0, \\ 1, & m_0 < m, \end{cases} \tag{45}$$

$$m_0 = \frac{\theta_1}{4r_\sigma\pi}(r_\sigma^2 + 4n^2\pi^2)^{\frac{1}{2}}, \tag{46}$$

and where θ_0 and θ_1 are defined in figure 2. The special form of $R_n(r)$ is determined in accord with the boundary conditions (25).

Substitution of (40) into (12)–(14) gives

$$U_{11} = -\sum_{m,n} R'_n(r)\, X^{(U)}_{mn}(\theta, z), \tag{47}$$

$$X^{(U)}_{mn} = \frac{1}{\gamma_m}\begin{cases} \exp[-\delta_{mn}z]\,(a_{mn}\sin\gamma_m\theta - b_{mn}\cos\gamma_m\theta), & m < m_0, \\ a_{mn}\sin\xi_{mn} - b_{mn}\cos\xi_{mn}, & m_0 < m, \end{cases} \tag{48}$$

$$V_{11} = -p_{11} - \rho_0 + V_{11H}, \quad V_{11H} = 2\sum_{m,n} R'_n(r)\, X^{(V)}_{mn}(\theta, z), \tag{49}$$

$$X_{mn}^{(V)} = -X_{mn}^{(p)}/\gamma_m^2, \tag{50}$$

$$W_{11} = -r\rho_0 - W_{11H}, \quad W_{11H} = \sum_{m,n} R_n(r)\, X_{mn}^{(W)}(\theta, z), \tag{51}$$

$$X_{mn}^{(W)} = -\frac{\delta_{mn}}{\gamma_m}\begin{cases}\exp[-\delta_{mn}z](a_{mn}\sin\gamma_m\theta - b_{mn}\cos\gamma_m\theta), & m < m_0,\\ a_{mn}\cos\xi_{mn} + b_{mn}\sin\xi_{mn}, & m_0 < m.\end{cases} \tag{52}$$

Substitution of (47), (49) and (51) into the shock conditions (32)–(34) shows us that U_{11H}, V_{11H} and W_{11H} are continuous across the shock front. We can, therefore, use the same system for the coefficients a_{mn} and b_{mn} without regard to the region with which we are concerned. We assume that h has a Fourier expansion in $0 \leqslant \theta \leqslant \theta_1$:

$$h(\theta) = \sum_{m=0}^{\infty}(a_{11m}\cos\gamma_m\theta + b_{11m}\sin\gamma_m\theta). \tag{53}$$

Substitution of (51) into (24) determines the coefficients as follows:

$$a_{mn} = a_{mn0}\cdot\begin{cases}b_{11m}, & m < m_0,\\ a_{11m}, & m_0 < m;\end{cases} \tag{54}$$

$$b_{mn} = a_{mn0}\cdot\begin{cases}(-a_{11m}), & m < m_0,\\ b_{11m}, & m_0 < m;\end{cases} \tag{55}$$

$$a_{mn0} = \frac{\gamma_m}{\delta_{mn}}\{(-1)^n e^{\frac{1}{2}r_\sigma} - 1\}\frac{16n\pi r_\sigma^2}{(r_\sigma^2 + 4n^2\pi^2)^2}. \tag{56}$$

To derive these statements we have used the orthogonality relations

$$\int_0^{r_\sigma} e^r R_n R_{n'} dr = \frac{r_\sigma^2 + 4n'^2\pi^2}{2r_\sigma}\delta_{nn'}, \tag{57}$$

and the integral relations

$$\int_0^{r_\sigma} e^r r R_{n'} dr = \frac{8n'\pi r_\sigma}{r_\sigma^2 + 4n'^2\pi^2}\{(-1)^{n'} e^{\frac{1}{2}r_\sigma} - 1\}. \tag{58}$$

Comparison of the problem of order ϵ_2 with the problem of order ϵ_1 readily gives

$$p_{12} = \rho_{12} = -2r\rho_0 + \tfrac{1}{2}\rho_0 + 2p_{11H}, \quad U_{12} = 2U_{11}, \tag{59), (60}$$

$$V_{12} = -p_{12} + r\rho_0 + 2V_{11H}, \quad W_{12} = -2r\rho_0 - 2W_{11H}. \tag{61), (62}$$

4. Addition theorem for the resultant drag on a system of scoops and numerical examples

Substitution of our scaling laws (1)–(5) into the drag formula

$$\bar{D} = 2\int_0^{\bar{\theta}_0}\int_{\bar{r}_0}^{r_\sigma}\bar{p}\sin\alpha\bar{r}\,d\bar{r}\,d\bar{\theta}, \tag{63}$$

where α is the inclination angle of a tangent to the cross-section of the scoop as shown in figure 2 and where $\bar{D}$ is the drag on a single scoop, gives us

$$\bar{D} = \frac{2\epsilon^2\bar{r}^2\bar{p}_{B0}}{G_0}\int_0^{\theta_0}\int_0^{r_\sigma}\exp(r + \tfrac{1}{2}\epsilon_2 r^2)\,p h_\theta\, dr\, d\theta. \tag{64}$$

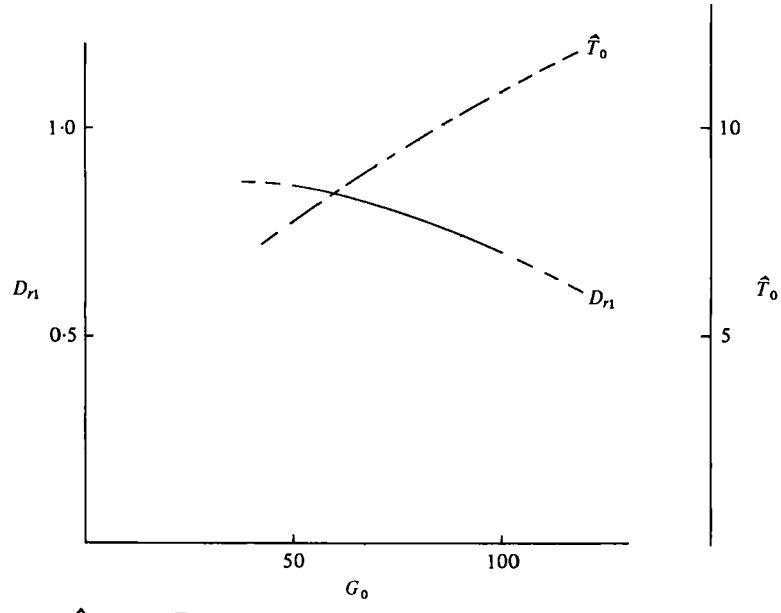

FIGURE 3. Factor $\hat{T}_0 = \epsilon_1\epsilon_3\bar{T}_0$ in (3) and D_{r1} in (65). The former gives us an idea about the temperature rise effected by the shock wave and the latter about the G_0-dependence of the scoop drag. Calculations are performed with $\epsilon_1 = 0{\cdot}07$, $\epsilon = 0{\cdot}05$, $\bar{T}_0 = 300$ and $(\bar{r}_\sigma - \bar{r}_0)\bar{r}_0^{-1} = 0{\cdot}05$.

Substitution of the solutions in § 3 into (64) gives

$$\bar{D} = \epsilon^2 G_{01}^{-1}\bar{r}_0^2\bar{p}_{BP}G_0^{\frac{3}{2}}D_{\theta 1}D_{r1}, \quad D_{\theta 1} = \int_0^{\bar{\theta}_0}(\partial\tilde{h}/\partial\bar{\theta})^2\,d\bar{\theta}, \tag{65), (66}$$

$$D_{r1} = \left(1+\frac{5\epsilon_1}{2}\right)\cdot\left(1+\epsilon_1+\frac{7\epsilon_2}{2}-r_\sigma(\epsilon_1+3\epsilon_2)-\frac{1+\epsilon_1+\frac{7}{2}\epsilon_2}{e^{r_\sigma+0{\cdot}5\epsilon_2 r_\sigma^4}}\right), \tag{67}$$

where for convenience we use the original azimuthal variable $\bar{\theta}$ to discuss the drag of a scoop with fixed aerofoil shape and $\bar{p}_{\mathrm{BP}}$ is the basic pressure on the outer cylinder. An important aspect of (65) is its independence of θ_1: In a system of many scoops, each scoop contributes to the total drag exactly the drag it would experience, did the system consist of that one scoop alone. The resultant drag of a system of scoops, therefore, is the drag of a standard system with a single scoop multiplied by the number of scoops. This simple addition theorem does not imply that the scoops fail to interact, for the velocity formulae in § 3 include θ_1 as a parameter. This fact clarifies the existence of the mutual interaction between scoops.

Figure 3 shows the factor D_{r1} as a function of G_0. The factor $\epsilon_1\epsilon_3\bar{T}_0$ is also given in figure 3. Calculations are performed with $\epsilon_1 = 0{\cdot}07$, $\epsilon = 0{\cdot}05$, $\bar{T}_0 = 300$ and

$$(\bar{r}_\sigma - \bar{r}_0)\bar{r}_0^{-1} = 0{\cdot}05.$$

The latter gives us an idea about the temperature rise behind the shock front.

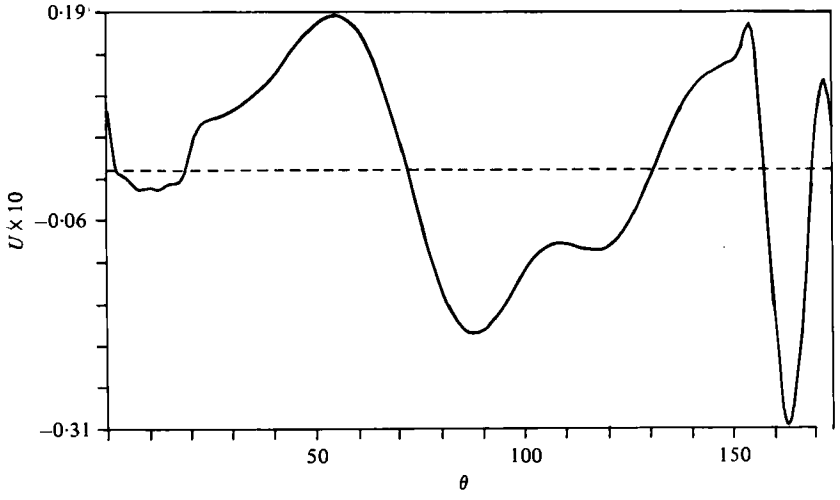

FIGURE 4. U_{11}-distribution of case 1 on the plane of symmetry $z = 0$ as a function of θ with $r = 0{\cdot}5$. The scoop profile is given as

$$W_0|_{z=0} = \begin{cases} \sin 2\pi\theta/\theta_0, & 0 \leqslant \theta \leqslant \theta_0, \\ 0, & \theta_0 \leqslant \theta \leqslant \theta_1, \end{cases}$$

with $\theta_0 = \pi/(10\sqrt{3})$ and $\theta_1 = \frac{1}{2}\pi$. The scaling unit of the abscissa is $\theta_0/20$.

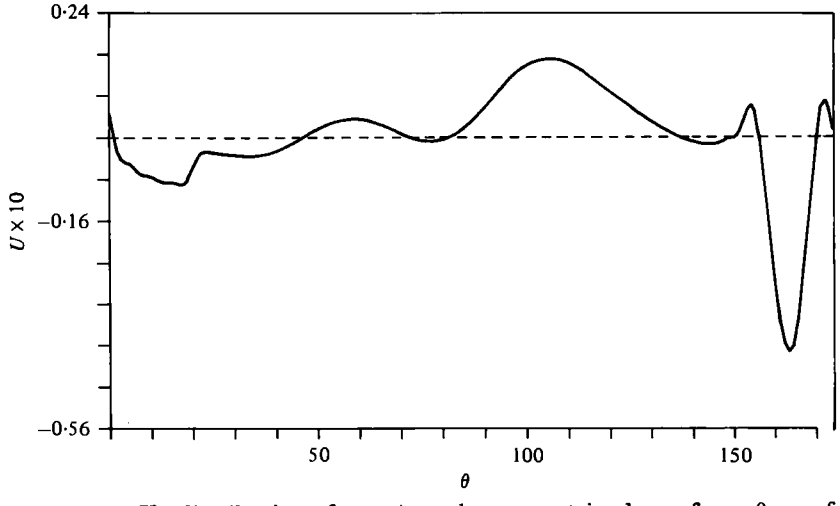

FIGURE 5. U_{11}-distribution of case 1 on the symmetric plane of $z = 0$ as a function of θ with $r = 2{\cdot}5$. The format of the figure is the same as in figure 4.

To gain an idea of the meridional flow, we calculate U_{11} and W_{11} for two cases in which

$$W_0|_{z=0} = \begin{cases} \sin 2\pi\theta/\theta_0, & 0 \leqslant \theta \leqslant \theta_0, \\ 0, & \theta_0 \leqslant \theta \leqslant \theta_1. \end{cases} \tag{68}$$

In the calculations, $r_\sigma = 5{\cdot}0$, $\theta_0 = \pi/(10\sqrt{3})$; in case 1, $\theta_1 = \frac{1}{2}\pi$, while in case 2, $\theta_1 = \frac{2}{3}\pi$. The double series (47) and (51) for U_{11} and W_{11} have been summed to the

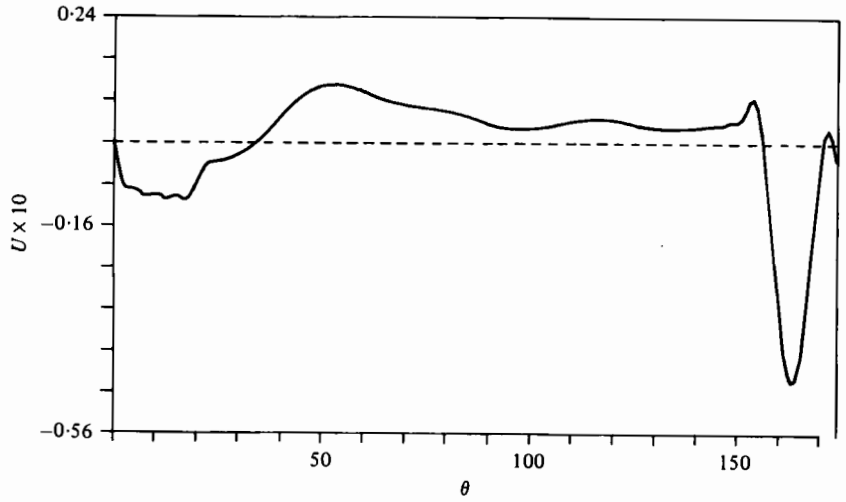

FIGURE 6. U_{11}-distribution of case 1 on the plane of symmetry $z = 0$ as a function of θ with $r = 4{\cdot}5$. The format of the figure is the same as in figure 4.

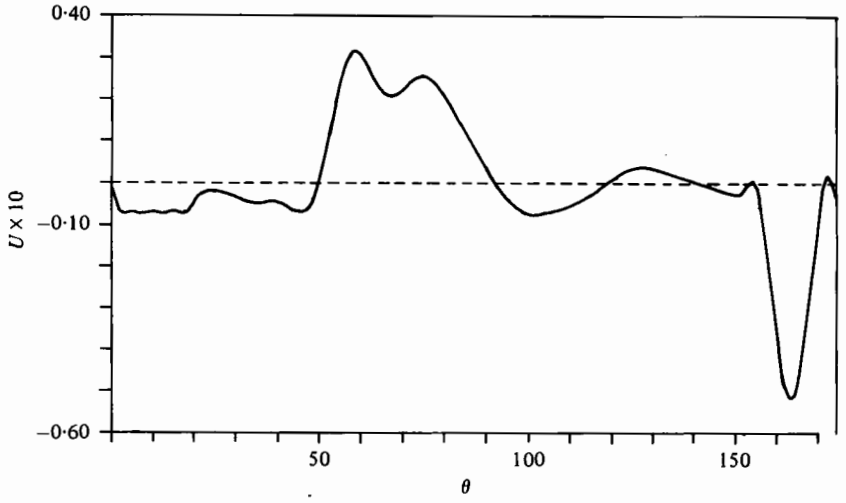

FIGURE 7. U_{11}-distribution of case 1 along a line of $z = 5{\cdot}0$ and $r = 2{\cdot}5$ as a function of $(\theta - 5{\cdot}0)$. The format of the figure is the same as in figure 4.

terms with $m = n = 35$; there was no appreciable difference from the results at $m = n = 25$.

Figures 4–6 give U_{11} in case 1 on the plane of symmetry $z = 0$ as functions of θ with $r = 0{\cdot}5$, $2{\cdot}5$ and $4{\cdot}5$, respectively. In a weakly hypersonic flow past a usual aerofoil, disturbances caused by the aerofoil propagate along Mach waves emanated from the aerofoil. As von Kármán's zone of action rule predicts, the aerofoil has no influence upstream. In a weakly hypersonic rotating flow past centrifuge scoops, the periodicity of the flow makes the upstream and the downstream parts interchange. Von Kármán's zone of action rule predicts an asymptotic radiation condition (28) far from the scoops. The space between scoops is full of disturbances caused by the scoops. This effect is

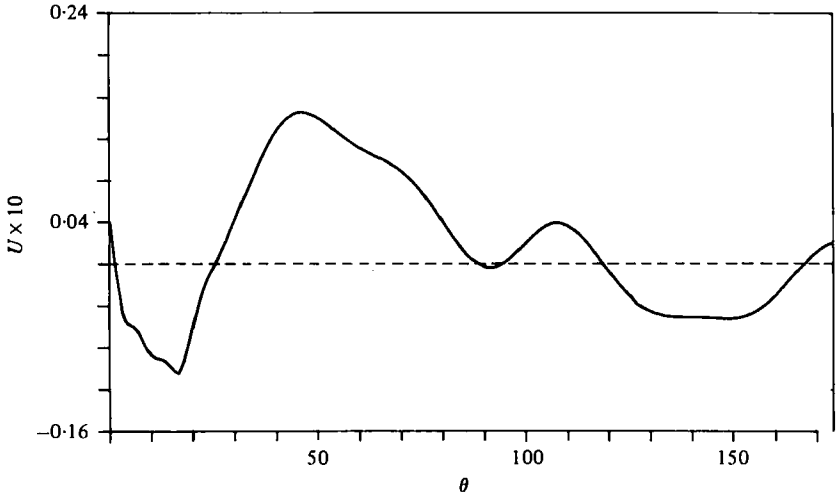

FIGURE 8. U_{11}-distribution of case 2 along a line of $z = 0$ and $r = 2{\cdot}5$ as a function of θ with the same scaling unit of θ as in figure 4. The scoop profile has the same analytic expression as in case 1 with the same value of θ_0 and with $\theta_1 = \frac{8}{9}\pi$. Because the abscissa extends only up to $\theta = \frac{1}{2}\pi$, a part of the flow field near the next scoop (i.e. the part with $\frac{1}{2}\pi \leqslant \theta \leqslant \frac{8}{9}\pi$) is discarded in this figure.

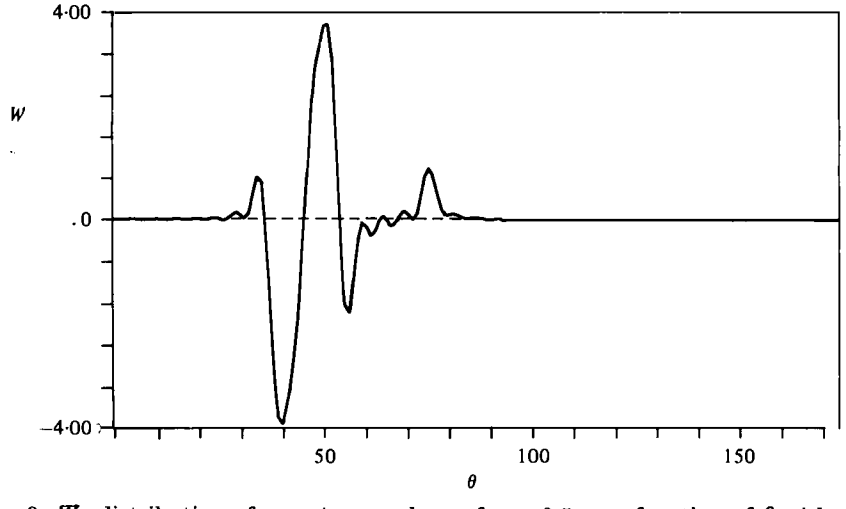

FIGURE 9. W_{11}-distribution of case 1 on a plane of $z = 0{\cdot}5$ as a function of θ with $r = 0$. The scaling unit is the same as in figure 4. Because the Mach wave emanated from the leading edge of the scoop is expressed as $\theta = z$, the Mach wave corresponds to the location of $\theta \sim 55$ in the figure.

shown dramatically in the figures 4–6. Figure 7 shows U_{11} in case 1 along the line $z = 5{\cdot}0$, $r = 2{\cdot}5$ as a function of $\theta - 5{\cdot}0$. We can recognize that properties of the U_{11}-configuration propagate along Mach waves with simultaneous modulation. Figure 8 gives U_{11} in case 2 along the line $z = 0$, $r = 2{\cdot}5$ as a function of θ with the same scaling unit as in case 1. As this figure makes clear, the flows in cases 1 and 2 are completely

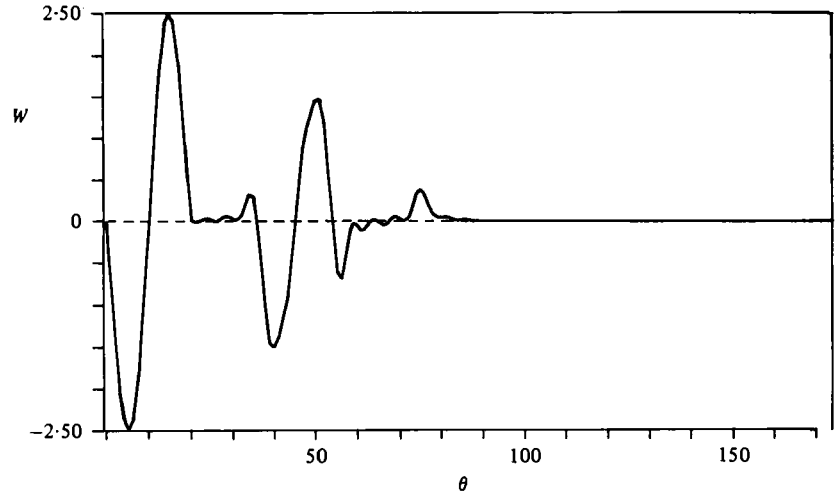

FIGURE 10. W_{11}-distribution of case 1 on a plane of $z = 0{\cdot}5$ as a function of θ with $r = 2{\cdot}5$. The format of the figure is the same as in figure 9.

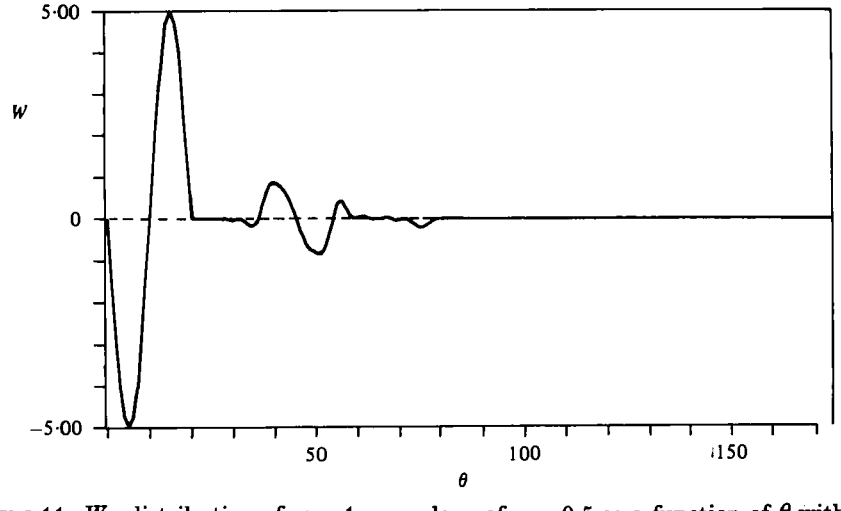

FIGURE 11. W_{11}-distribution of case 1 on a plane of $z = 0{\cdot}5$ as a function of θ with $r = 5{\cdot}0$. The format of the figure is the same as in figure 9.

different. There is mutual interaction between the scoops, despite our simple addition theorem.

Figures 9–11 give W_{11} in case 1 on the plane $z = 0{\cdot}5$ as functions of θ when $r = 0$, 2·5 and 5·0, respectively, with the same scaling unit of θ as in figure 4. Because the Mach wave from the leading edge is located on the plane $\theta = z$, the Mach wave corresponds to a location of $\theta \sim 55$ in these figures. We can again recognize appreciable disturbances in the space between the scoops. It is also interesting that the configuration on $r = 2{\cdot}5$ has a character combining those on the inner and the outer side walls. Figure 12 give W_{11} in case 1 along the line $z = 5{\cdot}0$, $r = 2{\cdot}5$ as a function of $\theta - 5{\cdot}0$. The figure makes it clear that the character of the W_{11} configuration propagates along

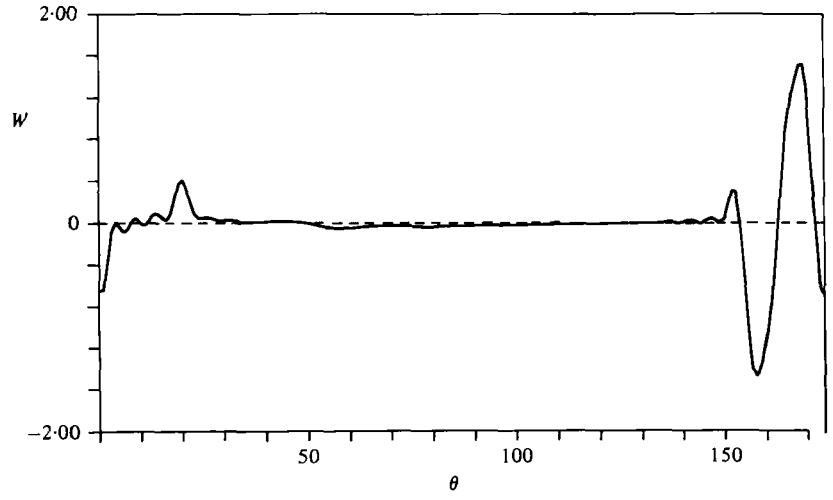

FIGURE 12. W_{11}-distribution of case 1 on line of $z = 5{\cdot}0$ and $r = 2{\cdot}5$ as a function of $\theta - 5{\cdot}0$. The format of the figure is the same as in figure 9.

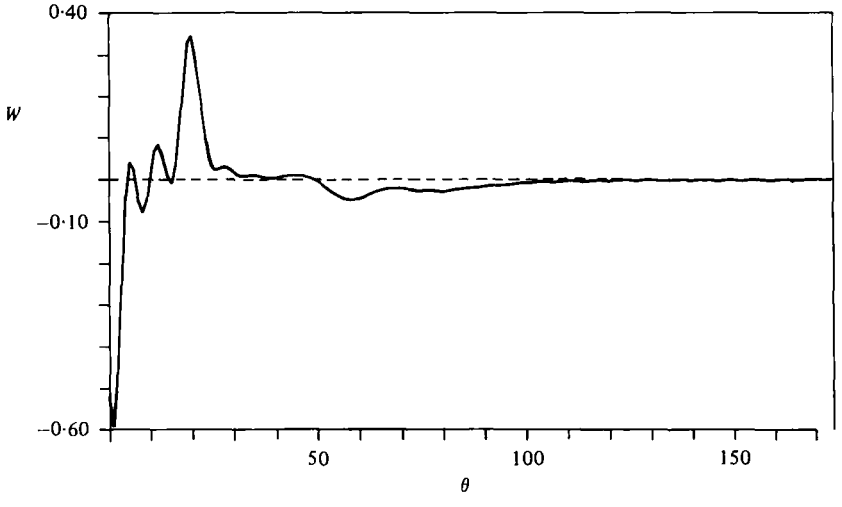

FIGURE 13. W_{11}-distribution of case 2 on line of $z = 5{\cdot}0$ and $r = 2{\cdot}5$ as a function of $\theta - 5{\cdot}0$. The scoop profile and the format of the figure is the same as in figure 8.

Mach waves with simultaneous modulation. The important point here is the fact that appreciable disturbances are localized in a narrow bundle of Mach waves and the remaining space between scoops remains relatively 'calm' as far as W_{11} is concerned. Figure 13, which gives W_{11} in case 2 along the line $z = 5{\cdot}0$, $r = 2{\cdot}5$ as a function of $\theta - 5{\cdot}0$ with the same scaling unit as in figure 4, also shows the existence of a similar bundle of Mach waves along which an appreciable disturbance in W_{11} propagates. To obtain the full expression for W, we must superpose upon W_{11} contributions from W_0. While the localization of appreciable axial disturbance, arising from the fact that W_0 itself is localized in a bundle of Mach waves bounded by the leading and the trailing Mach waves, may reflect our having applied a linearized theory, I believe this locali-

zation is physically correct. Because the above localization causes strong azimuthal variation of the axial flow, we must be careful not to interpret too literally the separation efficiency calculated on the assumption of axisymmetric axial flow.

The author expresses his thanks to Dr K. Hashimoto for helping to prepare the computer program for the automatic plotting schemes. He thanks also Dr M. E. McIntyre and the referees for their valuable suggestions and enlightening discussions, which helped him improve the presentation. He thanks finally Professor C. Truesdell for his valuable suggestions which helped him much to correct the presentation of the text.

Appendix

For the sake of clarity, exact statements of the basic equations, boundary conditions and shock conditions are given here. Also the derivation of the approximate equations is explained.

The equations refer to the rest frame of reference†

$$\frac{\partial\bar{\rho}}{\partial\bar{t}}+\frac{1}{\bar{r}}\frac{\partial\bar{r}\bar{\rho}\bar{q}_r}{\partial\bar{r}}+\frac{1}{\bar{r}}\frac{\partial\bar{\rho}\bar{q}_\theta}{\partial\bar{\theta}}+\frac{\partial\bar{\rho}\bar{q}_\theta}{\partial\bar{z}}=0, \tag{A 1}$$

$$\frac{D\bar{q}_r}{D\bar{t}}-\frac{\bar{q}_\theta^2}{\bar{r}}=-\frac{1}{\bar{\rho}}\frac{\partial\bar{p}}{\partial\bar{r}}, \quad \frac{D\bar{q}_\theta}{D\bar{t}}+\frac{\bar{q}_r\bar{q}_\theta}{\bar{r}}=-\frac{1}{\bar{\rho}\bar{r}}\frac{\partial\bar{p}}{\partial\bar{\theta}}, \tag{A 2), (A 3}$$

$$\frac{D\bar{q}_z}{D\bar{t}}=-\frac{1}{\bar{\rho}}\frac{\partial\bar{p}}{\partial\bar{z}}, \quad \frac{D\bar{E}}{D\bar{t}}-\frac{\bar{p}}{\bar{\rho}^2}\frac{D\bar{\rho}}{D\bar{t}}=0, \quad \bar{p}=\bar{\rho}\bar{R}\bar{T}, \tag{A 4), (A 5), (A 6}$$

where

$$\frac{D}{D\bar{t}}=\frac{\partial}{\partial\bar{t}}+\bar{q}_r\frac{\partial}{\partial\bar{r}}+\frac{\bar{q}_\theta}{\bar{r}}\frac{\partial}{\partial\bar{\theta}}+\bar{q}_z\frac{\partial}{\partial\bar{z}}, \tag{A 7}$$

and the other notations are used in the main text.

The boundary conditions are

$$\bar{q}_r\frac{\partial\bar{f}}{\partial\bar{r}}+\frac{\bar{q}_\theta}{\bar{r}}\frac{\partial\bar{f}}{\partial\bar{\theta}}+\bar{q}_z\frac{\partial\bar{f}}{\partial\bar{z}}=0 \quad \text{on each scoop}, \tag{A 8}$$

$$\bar{q}_r=0 \quad \text{on} \quad \bar{r}=\bar{r}_0 \text{ and } r_o[=\bar{r}_0(1+r_o\epsilon_2)], \tag{A 9}$$

where each scoop is expressed by

$$\bar{f}=\epsilon G_{01}^{-1}\bar{r}_0 h(\theta)-\bar{z}=0, \tag{A 10}$$

and $\bar{r}_0$ and $\bar{r}_o$ and the radius of the inner and the outer cylinders, respectively.

The shock conditions are

$$[\bar{\rho}\bar{q}_n]=[\bar{q}_{t1}]=[\bar{q}_{t2}]=[\bar{p}+\bar{\rho}\bar{q}_n^2]=[\bar{c}_p\bar{T}+\tfrac{1}{2}\bar{q}_n^2]=0 \quad \text{on the shock front}, \tag{A 11}$$

where the suffix n refers to the normal vector of the shock front, $t1$ and $t2$ to the two directions on the tangent plane of the shock front and square brackets to the jump of the bracketed quantity across the shock. The shocks are assumed to emanate from

† Because the scoops are at rest in a rigidly rotating 'free stream', this is the only kind of frame with respect to which the flow field can be steady.

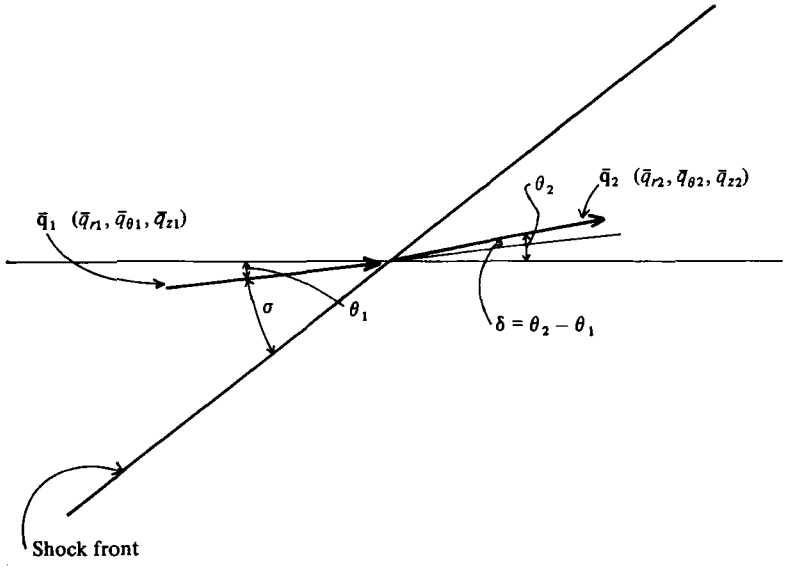

FIGURE 14. Local configuration of a shock front projected on the common tangent plane of $\mathbf{q}_1$ and $\mathbf{q}_2$.

the leading and the trailing edges of scoops (see figure 2) and the local configuration on a shock is sketched on figure 14.

Our problem is to solve (A 1) through (A 6) subject to boundary conditions (A 8) and (A 9) and shock conditions (A 11). Because of the scoop configuration as described in § 1 (see figure 1), the solution is expected to be periodic with respect to the azimuthal variable with period $\bar{\theta}_1$. We can restrict discussion to the flow field limited by bow waves of neighbouring scoops (see figure 2).

The approximate equations (7) through (21) and the boundary conditions (22) through (27) can be derived by straightforward substitution of the scaling laws (1) through (5) and the expansion formula (6) into (A 1) through (A 6), (A 8) and (A 9), then collecting terms of like powers in the expansion parameters. As for the shock conditions, we assume, in accord with our assumption that perturbations are small, that the difference between the shock angle and the Mach angle is small in comparison with the Mach angle. Substitution of the scaling laws (1) through (5) and the expansion formula (6), combined with the above assumption regarding the shock angle, into the shock conditions (A 11) give us (29) through (37).

REFERENCES

CHERNYI, G. G. 1961 *Introduction to Hypersonic Flow*. Academic.

CENEDESE, A. & CUNSOLO, D. 1979 Scoop optimal shape in a gas ultracentrifuge. In *Proc. 3rd Workshop on Gases in Strong Rotation, Rome, Italy* (ed. G. B. Scuricini), pp. 349–365. Comitato Nazionale Energia Nucleare.

ELSHOLZ, E. 1977 Die dreidimensionale Strömung in der Entnahmekammer einer Gaszentrifuge bei feststehendem Staukörper. *Rep.* DLR-FB-77-16.

HAYES, W. D. & PROBSTEIN, R. F. 1966 *Hypersonic Flow Theory*. Academic.

HULTGREN, L. S. 1978 Stability of axisymmetric gas flows in a rapidly rotating cylindrical container, pp. 173–200. Thesis, Massachusetts Institute of Technology.

JOHN, J. E. A. 1969 *Gas Dynamics*, pp. 29–33. Boston: Allen and Bacon.

LANDAHL, M. T. 1977 Boundary layers and shear layers in a rapidly rotating gas. In *Proc. 2nd Workshop on Gases in Strong Rotation, Cadarache, France* (ed. Soubbaramayer), pp. 15–50. Centre d'Etude Nucleaires de Saclay.

MATSUDA, T. & HASHIMOTO, K. 1976 Thermally, mechanically or externally driven flow in a gas centrifuge with insulated horizontal end plates. *J. Fluid Mech.* **78**, 337–354.

SCHMIDT, W. VON 1972 Strömungsmodell von Gegenstrom – Gasultrazentrifugen. *Atomkernenergie* **20**, 299–303.

SUZUKI, M. & MIKAMI, H. 1979 Pitot-tube measurement of the flow of a rotating gas behind a stationary cylinder. In *Proc. 3rd Workshop on Gases in Strong Rotation, Rome, Italy* (ed. G. B. Scuricini), pp. 481–507. Comitato Nazionale Energia Nucleare.

WARD, G. N. 1955 *Linearised Theory of Steady High-Speed Flow*. Cambridge University Press.

ZIPPE, G. 1960 The development of short bowl ultracentrifuges. *Div. Engng Phys., Res. Lab. Engng Sci., Univ. of Virginia Rep.* no. EP-4420-101-60U.